Flotation study of fine grained carbonaceous sedimentary apatite ore – Challenges in process mineralogy and impact of hydrodynamics

Hoang, D. H.; Kupka, N.; Peuker, U. A.; Rudolph, M.;

Originally published:

March 2018

Minerals Engineering 121(2018), 196-204

DOI: https://doi.org/10.1016/j.mineng.2018.03.021

Flotation study of a fine grained carbonaceous sedimentary apatite ore – challenges in process mineralogy and impact of hydrodynamics

Duong Huu Hoang[1,2,3], Nathalie Kupka[3], Urs Alexander Peuker[2], Martin Rudolph[3]

[1]Department of Mineral Processing, Faculty of Mining, Hanoi University of Mining and Geology, Duc Thang, Bac Tu Liem, Hanoi, Vietnam

[2]Institute of Mechanical Process Engineering and Mineral Processing, TU Bergakademie Freiberg, Agricolastraße 1, Freiberg, Germany

[3]Department of Processing, Helmholtz-Institute Freiberg for Resource Technology, Helmholtz-Zentrum Dresden-Rossendorf, Chemnitzer Straße 40, Freiberg, Germany

ABSTRACT

The flotation beneficiation of apatite for phosphate production is challenging for finely disseminated sedimentary ores rich in carbonates. Similarities in surface properties of the semi-soluble salt-type carbonate and phosphate calcium minerals combined with fine intergrowth are the main reasons for poor grade and low recoveries. Imperfect depression of the calcium/magnesium carbonate minerals, e.g. calcite and dolomite, will lead to weakly hydrophobic surface properties and thus true flotation of this gangue. Furthermore, the fine particles, necessary for sufficient mineral liberation, strongly affect the bubble-particle collection due to negative rheological effects within the pulp with a decrease in the flotation kinetics of the fine valuables and an increase in entrainment of fine gangue particles.

This study presents the results and discussions based on automated mineralogy (MLA) size-by-size-by-liberation analyses for various mineral groups. In addition, we present results on different turbulent hydrodynamic parameters based on various tests in a lab cell and discuss the discrepancies from fundamental modeling results.

KEYWORDS

Carbonaceous sedimentary apatite; Automated mineralogy (MLA); Surface liberation; Turbulent hydrodynamics; Flotation kinetics

1 Introduction

Phosphate rock is the primary source of phosphorus, i.e. the production of phosphoric acid used in agricultural fertilizers, pharmaceuticals, cosmetics and the chemical industry in general. The world's demand for fertilizers is expected to continuously increase due to the population growth. The demand for phosphate fertilizers (P_2O_5) is forecasted to grow annually by 2.2 % from 2015 to 2020 [1].

Sedimentary phosphate ores make up approximately 80 % of the world's total phosphate rock production [2, 3]. Typical gangue minerals associated with these reverses include carbonates (dolomite, calcite and ankerite), clays and silica. The beneficiation process becomes more difficult in the presence of significant amounts of carbonate minerals with fine intergrowth. Many separation methods have been investigated, but there is still no widely accepted economic efficient methods for separating carbonate from phosphate ores [4].

1.1 Challenges in selectivity for carbonates and phosphates

Froth flotation is considered as the most effective process for the beneficiation of the sedimentary phosphate ore, with more than 60% of the marketable phosphate in the world being processed by flotation [5]. For carbonaceous sedimentary phosphate ores, flotation is facing various challenges due to mineralogical surface property similarities between carbonate and phosphate minerals. The carbonaceous sedimentary phosphate ores contain similar constituent minerals such as calcium/magnesium carbonates and calcium phosphate, which results in similar surface properties. All minerals apatite ($Ca_{10}(PO_4)_6F_2$), dolomite ($CaMg(CO_3)_2$) and calcite ($CaCO_3$) belong to the group of semi-soluble salt-type minerals containing similar cations (Ca^{2+})[4].

Apatite, dolomite and calcite minerals are sparingly soluble in aqueous solutions and will release their lattice constituents into the solution. Sedimentary carbonaceous ores contain a significant amount of $(CO_3)^{-2}$ and F^- substituted for $(PO_4)^{-3}$, along with the cationic substitutions of Mg^{2+} for Ca^{2+} [4, 6, 7]. These dissolved ions and their species forming in solution depending on solution thermodynamics can also interact with various minerals surface changing their properties to interact with various reagents (collector, depressant) added. Such interactions are the main reason for poor reagent adsorption selectivity [8]. Solution thermodynamics of systems containing various suspended semi-soluble salt-type minerals with high surface areas in combination with dissolved flotation reagents are rather complex. In addition to the dissolution of minerals and adsorption of dissolved mineral and

reagent species at the interface, interactions between these species in the bulk can lead to complicated phenomena such as surface and bulk precipitation as well as re-dissolution of adsorbed species [8]. Due to a surface reaction, the lattice is disrupted and a new phase is formed, surface precipitation may occur in the interfacial region [9].

Competition of the dissolved mineral species with similarly charged collector species for adsorption sites can result in the depression. The reagents (collector, depressant) interact with the exposed surface of phosphates and also interact with carbonate minerals which have weakly hydrophobic surface properties, leading to true flotation of this gangue.

1.2 Challenges of fine particle flotation – impact of turbulent hydrodynamics

There are a number of further unfavorable properties of sedimentary phosphate ores not mentioned above, including [4]:

- *High slimes production:* Because of the soft nature of sedimentary phosphate ore, specifically the softer dolomite-rich pebbles, large amounts of slimes are produced during the comminution and the conditioning stage. This can significantly increase reagent consumption while reducing the selectivity of the flotation process [10].

- *Porous nature of sedimentary phosphates.* Sedimentary phosphate particles are typically made up of very small mineral grains, which results in micron-sized pores. These "micropores" can significantly increase total surface area of the particles and increase reagent consumption [11, 12]

- *Very fine liberation size.* Phosphate particles can contain fine (micron to submicron-sized) dolomite inclusions. Grinding to such a size as to liberate the fine dolomite inclusions would significantly reduce selectivity of flotation processes [11-13]

In addition, the fine particles, necessary for sufficient mineral liberation strongly affect the bubble-particle collection (i.e. collision and attachment) due to negative rheological effects within the pulp with a decrease in the flotation kinetics of the fine valuables (affecting the recovery) and an increase in entrainment of fine gangue particles (affecting the grade). The main reason for poor recovery is the low frequency of collision between particles and bubbles Z_{PB} [14-17]. Fine particle due to their small size and consequently small mass rather follow fluid streamlines around air bubbles than to collide with them. Hence, the efficiency of collision E_c is set in relation to the ratio of particle size and bubble size [15, 16, 18].

$$E_c = \tanh^2\left[\sqrt{\frac{3}{2}.\left(1+\frac{3/16.\mathrm{Re}}{1+0.249.\mathrm{Re}^{0.56}}\right)}\left(\frac{d_p}{d_b}\right)\right]$$ *[19-22]* *(Eq. 1)*

Collision probability is governed by the physics of the process (or hydrodynamics), while attachment probability and stability of attachment include a chemical component (particle hydrophobicity) [23]. Therefore, optimization of turbulence hydrodynamics in flotation cell plays a very important role, especially for fine particle flotation.

In this study, automated mineralogy (MLA) is applied on size-by-size-by-liberation classes to obtain a better understanding of the effect of size, liberation and various mineral groups on the flotation performance. In addition, the effects of different turbulent hydrodynamic parameters are being investigated in order to determine the role of turbulence in fine particle flotation.

2 Materials and methods

2.1 Ore

The apatite samples for this study were provided by the Vietnam Apatite Limited Company. Detailed information of the sample preparation procedures can be found in [24, 25]. The apatite samples after 8 minutes grinding (particle size distribution parameters $D_{10,3}$ = 5.3 µm, $D_{50,3}$ = 27.9 µm, and $D_{90,3}$ = 67.1 µm) were used for flotation tests. All the samples (four size fractions of feed, tailings and four subconcentrates) were sent for chemical assay by ICP-OES and Mineral Liberation Analysis (MLA).

2.2 Reagents

Sodium hydroxide: NaOH with chemical analysis grade having the purity ≥ 99%. It was supplied by Carl Roth GmbH & Co. KG, Germany and used as received.

Sodium carbonate: Na_2CO_3 99.9 % was bought from VWR Company, Belgium. It is applied as a pH modifier to achieve alkaline environment. A two percent solution was prepared for application.

Sodium silicate: Na_2SiO_3 has the purity of 99 % was supplied by Zschimmer & Schwarz GmbH & Co. KG, Germany.

Corn starch: $(C_6H_{10}O_5)_n$ was supplied by Carl Roth GmbH + Co. KG, Germany. It is gelatinized with NaOH at a 4/1 ratio Starch/NaOH, was used as carbonate depressant.

Methyl isobutyl carbinol: MIBC was used as a frother, provided by Sigma-Aldrich, Germany.

The collector is Berol 2015, a formulation of an amphoteric collector and a nonionic secondary collector supplied by AkzoNobel Surface Chemistry, Sweden. Berol 2015 is intended to be used as a collector for the flotation of oxide and salt type minerals such as apatite, scheelite and fluorspar.

2.3 Lab flotation procedure

The batch flotation tests are performed using an MVTAT flotation cell self-made at the TU Bergakademie Freiberg. In order to minimize the impact of froth recovery, the flotation test was developed by using shallow froth levels and frequent froth removal [26]. **Figure 1** provides an overview of the flotation process and reagent regimes.

Four sub-concentrates were taken, C1 (0 - 0.75 min), C2 (0.75 - 1.5 min), C3 (1.5 – 3 min), C4 (3 – 6 min). After completion of the flotation tests, the concentrate and the tailings products were filtered, dried, weighed and analyzed.

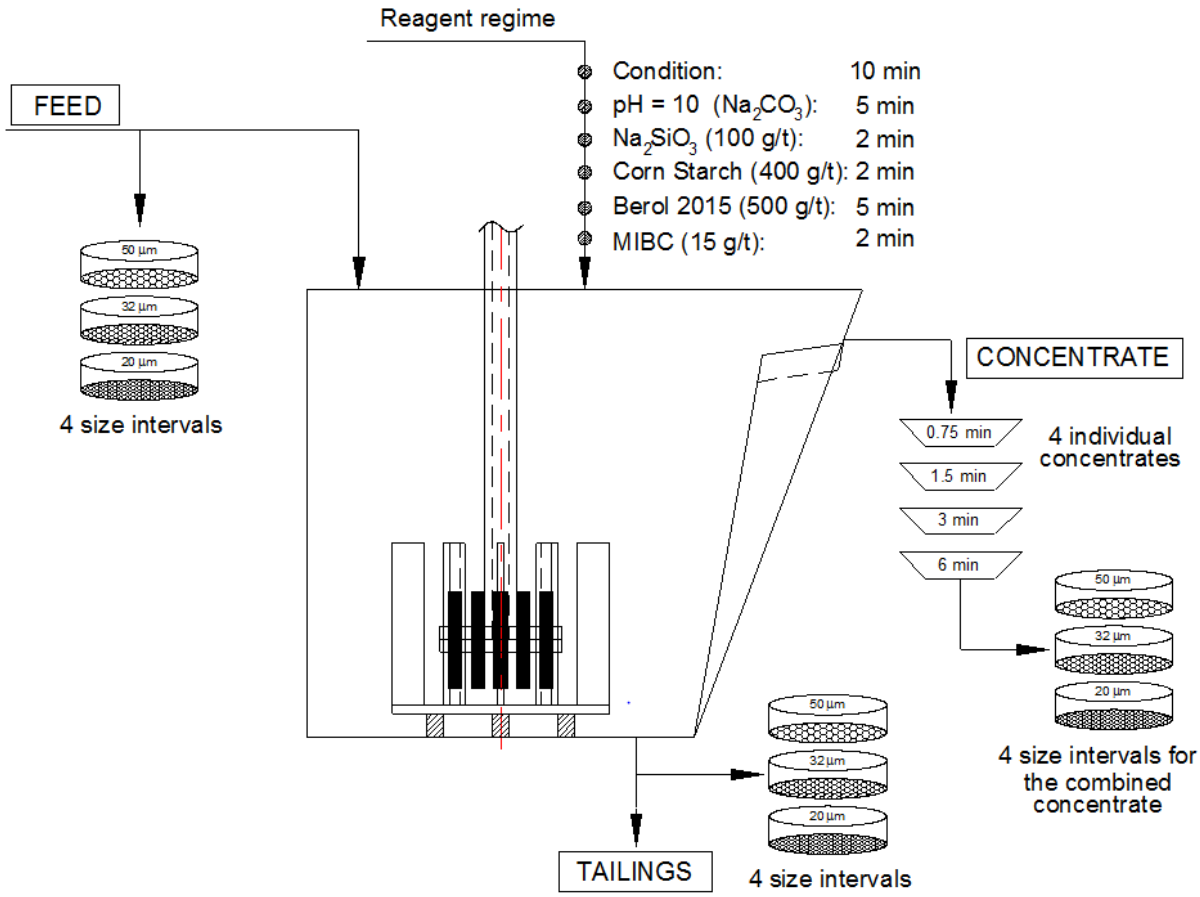

Figure 1. *Complete flotation process (following the MinnovEX Flotation test procedure [26]*

The flotation tests were conducted in five replicates to be left with sufficient sample mass of the different streams for characterizing the sample.

2.4 Chemical assay – ICP-OES

The feed, un-sized flotation products and tailings and all the size-by-size sub-samples after sieving were taken as representative samples for chemical assays using ICP-OES. The sample was digested in 8 ml of acid composed of hydrochloric and nitric acid in a molar ratio of 3:1 (aqua regia). The solution was boiled at 70 °C on a hot plate until the reaction was complete (about 1 h). After that it was allowed to settle in a flask for approximately 12 h. Afterwards, the entire solution was transferred into a 500 ml volumetric flask and de-ionized water is added to bring the solution to the final volume. A 15 ml of this dilution was used for ICP-OES measurements. The standard sample concentrations were measured from time to time in the course of the analyses to check the accuracy of the calibration curve. Five replicates were taken and averaged for each element. The wavelengths used were as follows: Ca 318.1 nm; Mg 279.0 nm and P 213.6 nm.

2.5 Automated Mineralogy (MLA)

Twenty-four samples of all the size-by-size sub-samples for the feed, concentrates and tailings were handed to the automated mineralogy (Mineral Liberation Analyzer, MLA).

The sample preparation process is provided by Leissner et al. [24, 25]. More detailed information on the functionality of the MLA system can be found in [27, 28]. A description of the exact analytical procedure is provided by Sandmann and Gutzmer [29].

During the screening of the samples, special care was taken to avoid agglomeration of the particles, which would potentially have caused biased results in both the particle size distribution and the MLA measurements. The MLA measurements were carried out at the Geometallurgy Laboratory of the Helmholtz Institute Freiberg for Resource Technology, Freiberg, Germany.

Evaluation of MLA measurements provides information on the qualitative and quantitative mineralogy as well as the grain size distribution and mineral liberation by volume and surface. In this study, grain size distributions and liberations are the main attributes assessed. Data processed with the mineral liberation analyzer does not comprise stereological transformation. If there is written about liberation, it is always related to the pure two-dimensional data.

3 Results and discussions

3.1 Automated Mineralogy and Chemical Analyses

The particle size distribution of the feed sample comparing different methods shows a good correlation with low standard deviations (cf. **Figure 2b**). The particle size results from wet sieving of the feed sample, four concentrates and tailings is given in **Figure 2a**. The amount of fine particles (0 – 20 µm) increases with flotation time, this can be attributed by a change of the collision efficiency E_c, i.e. the fine fraction is floating more slowly. In the same condition (liberation degree, rheological properties of the pulp), E_c is a function of the particle/bubble size ratio (eq. 1), so the coarser particles have a higher chance to collide with the bubbles.

Furthermore, the froth structure is significantly changed after the removal of large amounts of material. This might also affect the recovery of fine particles through entrainment.

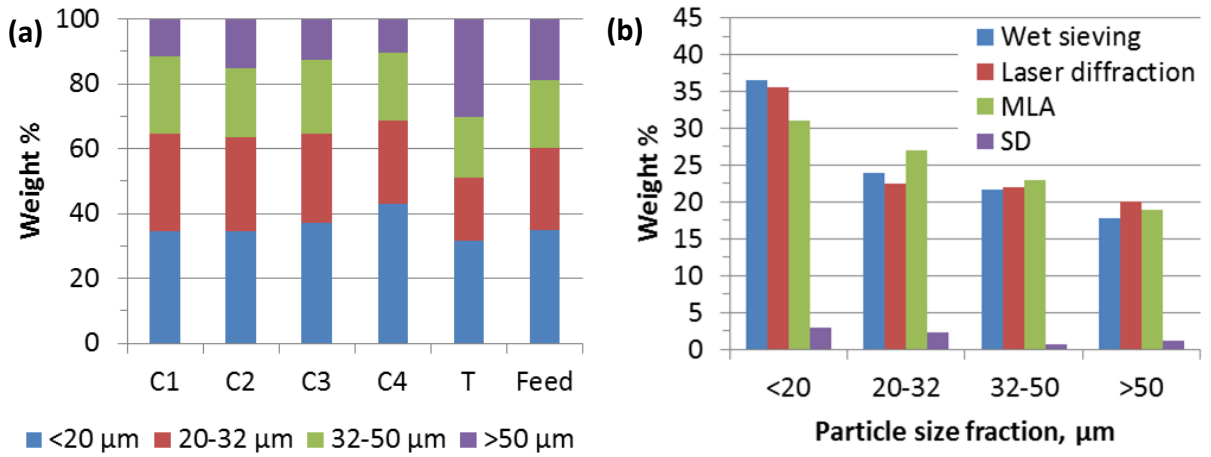

Figure 2. *(**a**) Weight percentages of size classes of concentrates and tailings after flotation, (**b**) Comparison of different methods with standard deviation SD*

3.1.1 Mineral Composition

The main constituents of the feed sample are apatite (64 % by weight), carbonate minerals (27 %), silicates (8 %) and 1 % other minerals. The results show the 20 - 32 µm size class containing the highest amount of apatite, and a low grade in coarse particles (> 50 µm) which contains a high amount of silicates (cf. **Figure 3**).

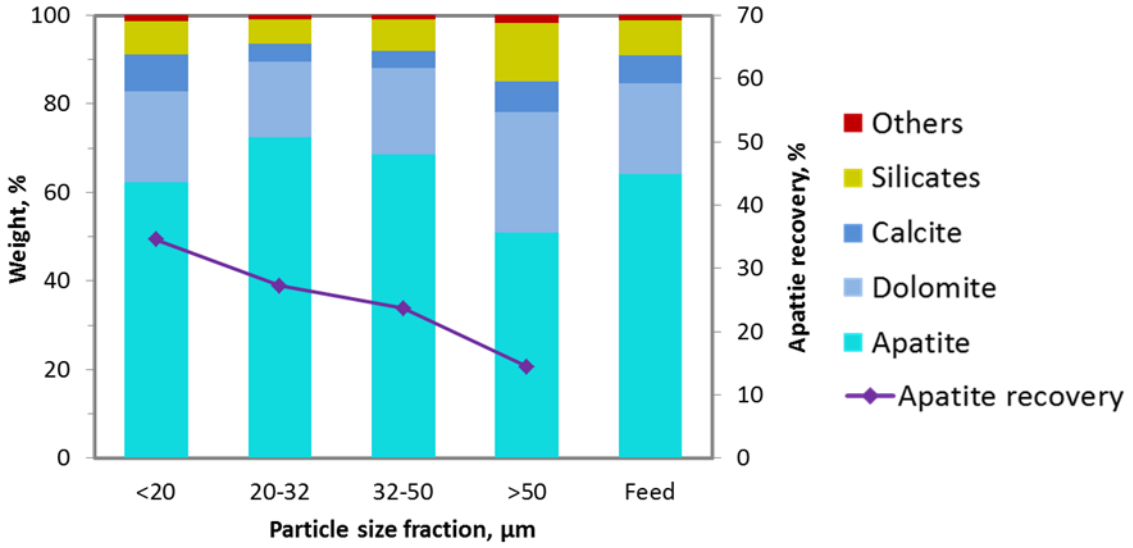

Figure 3. *Mineral composition of the feed sample and four size classes as determined with MLA*

3.1.2 Comparison of chemical assay and mineral liberation measurements

Assays of duplicate representative sub-samples were performed for all unsized and size-by-size sub-samples of the feed, concentrates and tailings. The results of the chemical assay by ICP-OES and MLA measurements of all sub-samples are presented in **Figure 4**.

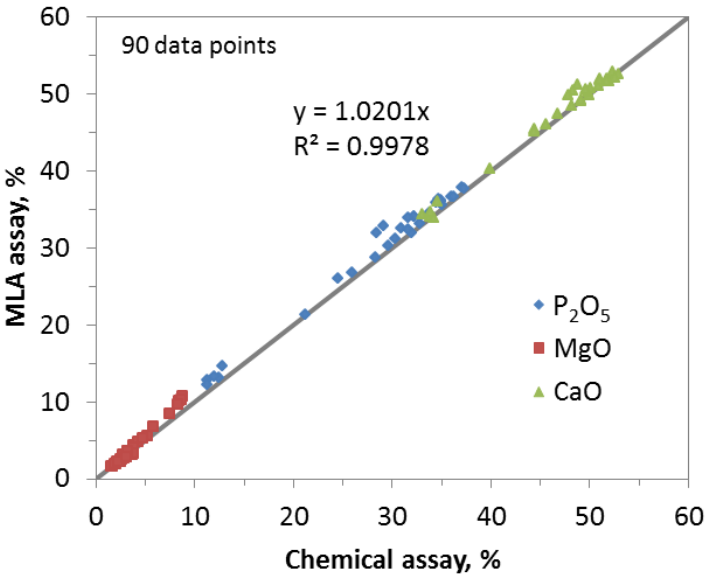

Figure 4. *Comparison between grade of P_2O_5 (corresponds to apatite), MgO (corresponds to dolomite) and CaO as calculated from chemical assays (ICP-OES) and from MLA measurements*

The data shows a good correlation between the measurements using the two different techniques, demonstrating that the MLA was able to differentiate adequately the three major mineral phases in the carbonaceous apatite ore. It can be seen that the MLA

calculated assays compare very well with the chemical assays, giving confidence in the MLA measurement. However, the MLA assay is mostly higher than the corresponding ICP-OES assay due to there are still many unpreventable agglomerates forming in the MLA samples, especially, for fine particles. This leads to increase the mineral surface and will affect on mineral surface liberation.

3.1.3 Mineral Associations

The mineral association results from MLA are given in **Figure 5a**. The main gangue interlocked with apatite is carbonate minerals (dolomite and calcite), whereas dolomite has the highest value. The amount of locked particles increases with particle size, i.e. liberation by free surface of apatite decreases with increasing particle size.

Figure 5b shows that dolomite is associated mainly with apatite. The relationship between dolomite recovery and surface liberation is given in **Figure 7**.

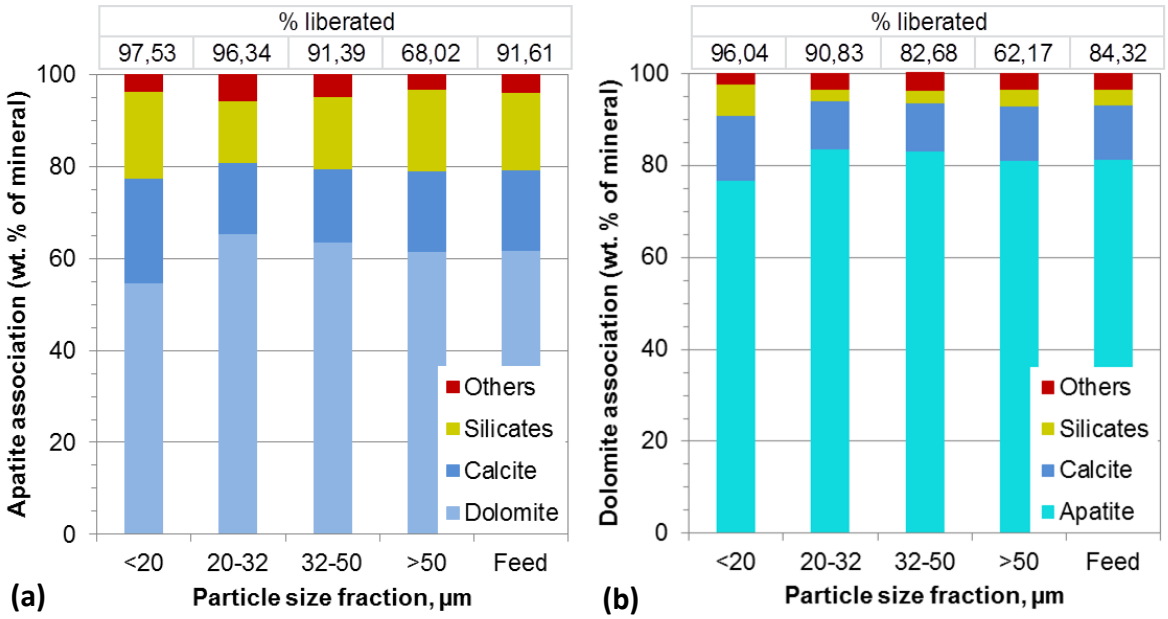

Figure 5. a) *Apatite association* ***b)*** *Dolomite associated with other minerals* $(Mineral\ association = \frac{\%\ mineral\ surface}{100-\%\ free\ surface} * 100)$

3.2 Size-by-size by liberation analysis for different mineral groups

3.2.1 Apatite

The liberation by free surface refers to the analysis of the exposed surface of particles containing a given grain mineral. In order to evaluate the liberation by free surface,

liberation classes were defined as: 0 – 60 %, 60 – 85 %, 85 – 100 % and 100 %, which aim to have approximately the same number of the target mineral particles present in each liberation classes.

Figure 6 shows the apatite recovery kinetics of different particles size fractions and for different surface liberation classes. The apatite recovery increases with the increasing % free surface of apatite in the same particle size fraction. However, due to unpreventable agglomerates forming in the MLA samples, the recovery of the size fraction 0 - 20 µm at 100 % free surface seem lower than for medium surface liberations at the beginning of flotation, hence it is assumed to be an analytical artifact. Hence, for such fine particle fractions, there need to be further developments in the sample preparation to prevent agglomerate formation.

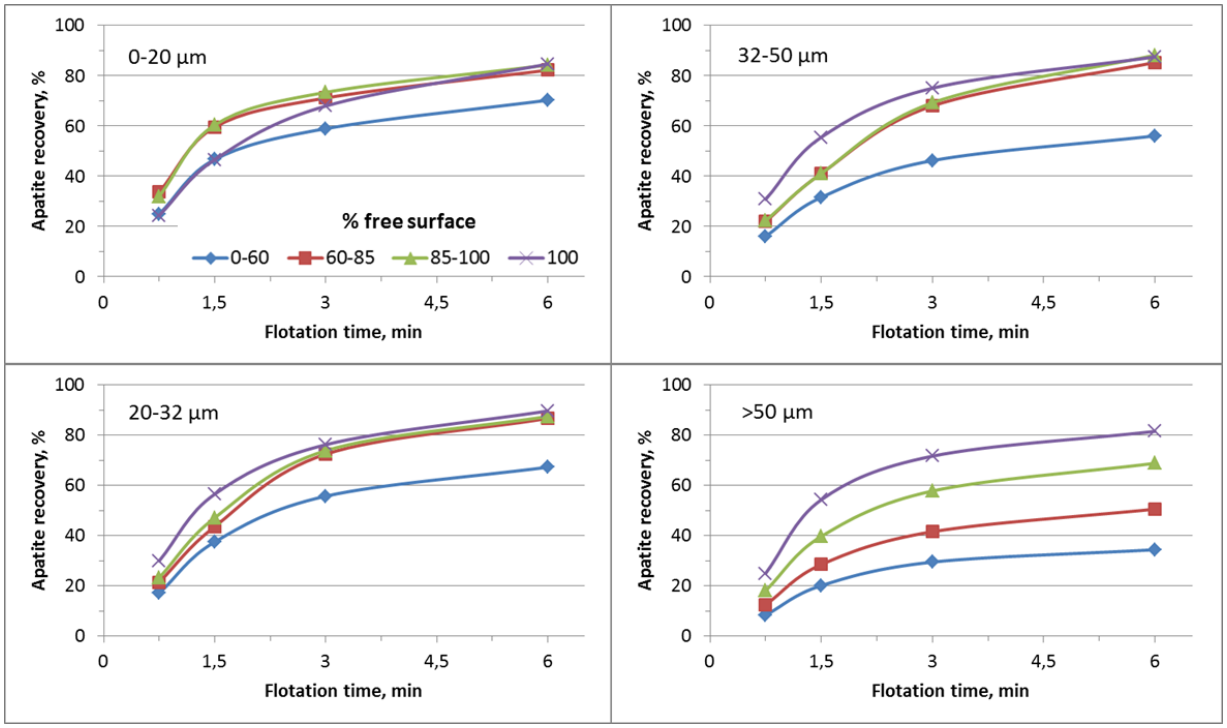

Figure 6. *Apatite recovery by size and liberation classes*

In addition, it can be seen that the 60 - 85 % and 85 - 100 % surface liberation have very similar behavior. This is very important, because the liberation only needs to be at 60 - 85 % to allow proper flotation. In cases where only a high apatite recovery is considered, fine grinding might not be necessary, the comminution and flotation processes could be following two steps: primary flotation then a regrinding and a second flotation. Of course, this poses other challenges, e.g. finely disseminated gangue.

3.2.2 Carbonaceous Gangue

Carbonate minerals (dolomite and calcite) are the main gangue and have similar physical properties to apatite and are associated with apatite. The behaviour of dolomite and calcite being very similar, in this study we will just present the results for dolomite.

As the surface liberation of dolomite increases, its recovery decreases (cf. **Figure 7**). Fully liberated carbonate minerals (100% free surface) can be floated, in this case it must be true flotation of this carbonate gangue. However, dolomite floats better when it is associated with apatite and poorer when fully liberated. This also shows that the reagents are rather selective towards apatite, especially Berol 2015 in combination with the depressants used.

In addition, the particle size and % free surface have a pronounced effect on the recovery, the recoveries of carbonate minerals increases as particle size or % free surface decreases. Dolomite is associated mainly with apatite (cf. **Figure 5b**), thus, a lower surface liberation will lead to higher recoveries through association.

Unlike apatite, the effect of liberation class is more important for dolomite: 60 – 85 % and 85-100 % do not have the same behaviour. Dolomite is finely intergrown with apatite, hence fine grinding is necessary to separate dolomite by flotation [25].

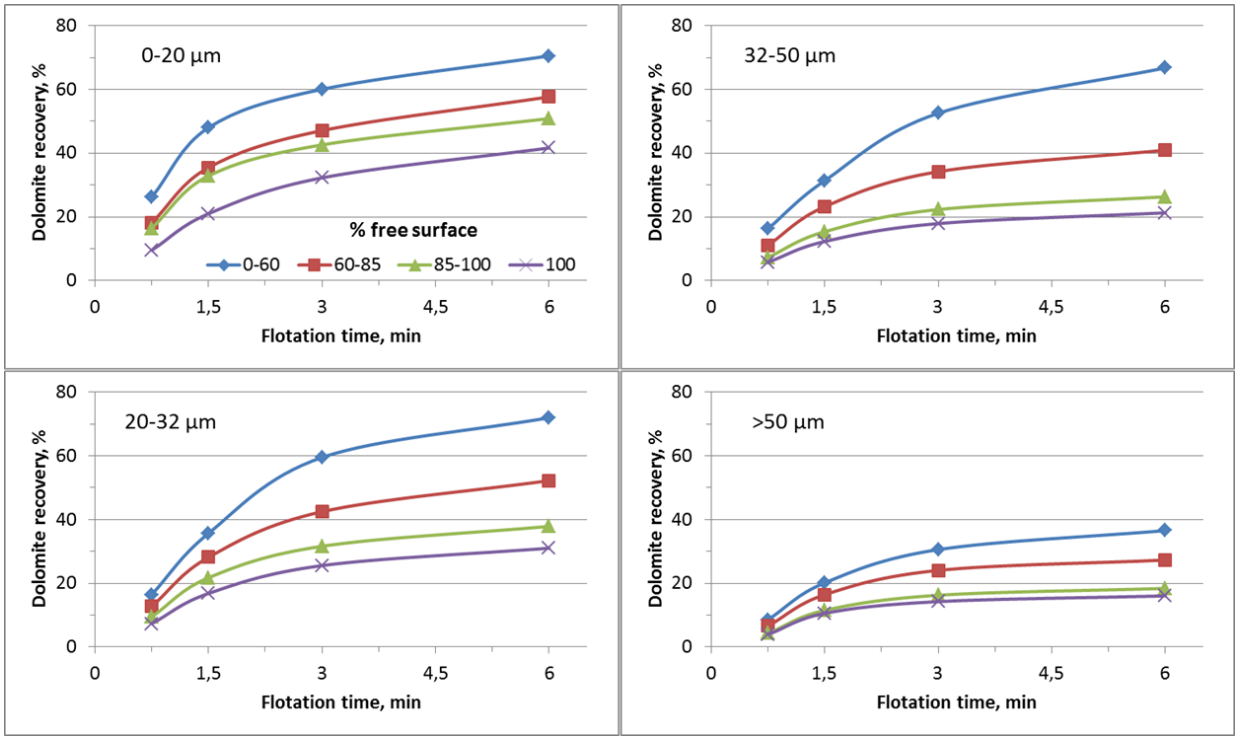

Figure 7. *Dolomite recovery by size and liberation classes*

3.2.3 Siliceous Gangue

The siliceous minerals group is selected because they are considered as truly hydrophilic silicate minerals, i.e. quartz, phlogopite, plagioclase, albite, orthoclase, sanidine, almandine, zircon, titanite, muscovite. Similarly to carbonate minerals, silicates are associated with mainly apatite and only minor amounts of dolomite and calcite. **Figure 8** shows that the silicates recovery decreases as % free surface increases. The recovery of fully liberated particles increases as the particle size decreases, therefore, said fully liberated silicate particles can only end up in the concentrate because of entrainment.

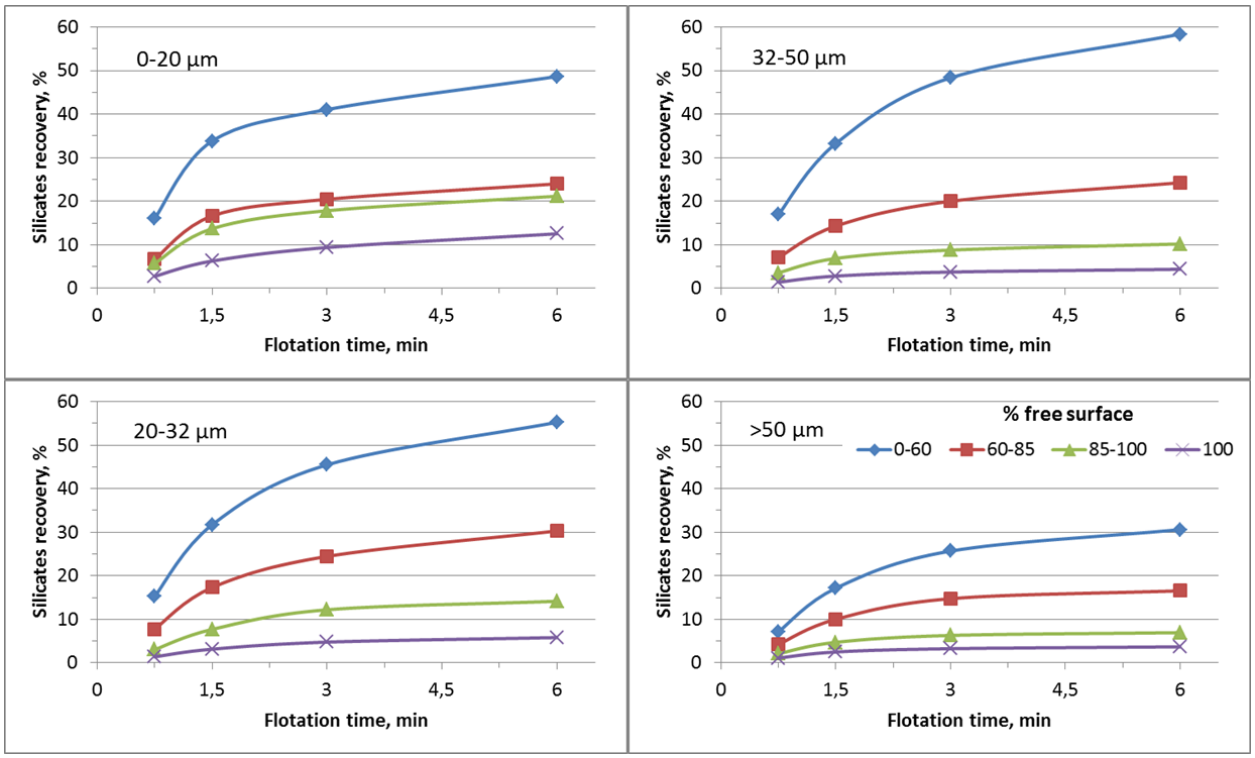

Figure 8. *Silicates recovery by size and liberation classes*

3.2.4 Effect of mineral hydrophobicity and size on the recovery

The recovery of carbonate minerals also increases with particle size, however less than for apatite, as their overall rate constants are considerably lower than apatite's. This indicates that the carbonaceous phosphate ores are a complex system and is therefore difficult to separate carbonates with conventional froth flotation.

Figure 9 illustrates four types of recovery-size relationships for different hydrophobicity minerals. The results are in good agreement with Wills and Finch [23]. For the strongly floatable mineral (apatite) there is a broad intermediate size range (20-32 µm) of highest recovery. The less floatable minerals (dolomite and calcite) are strongly dependent on the particle size, showing an increase in the recovery as particle size decreases. This can be due

to the different solubilization kinetics of finer particles and leading to adsorption of collector molecules and thus hydrophobization. It could as well be due to reduced electric double layer repulsion between small carbonate particles with higher solubility and the gas bubbles. Both effects could occur simultaneously and account for the increase in flotability of these particle fractions. The silicates (hydrophilic minerals) are assumed to mainly be recovered by entrainment with a typical shape curve. The above discussed principal mechanisms of flotation of fine particles, e.g. entrainment is the reason for reduced selectivity of separation in the fraction below 20 µm.

The size-by-size recovery shows the typical optimal size range of recovery found in the literature [17, 30-32], with intermediate particles having highest recovery and lower values for the finer and coarser sizes.

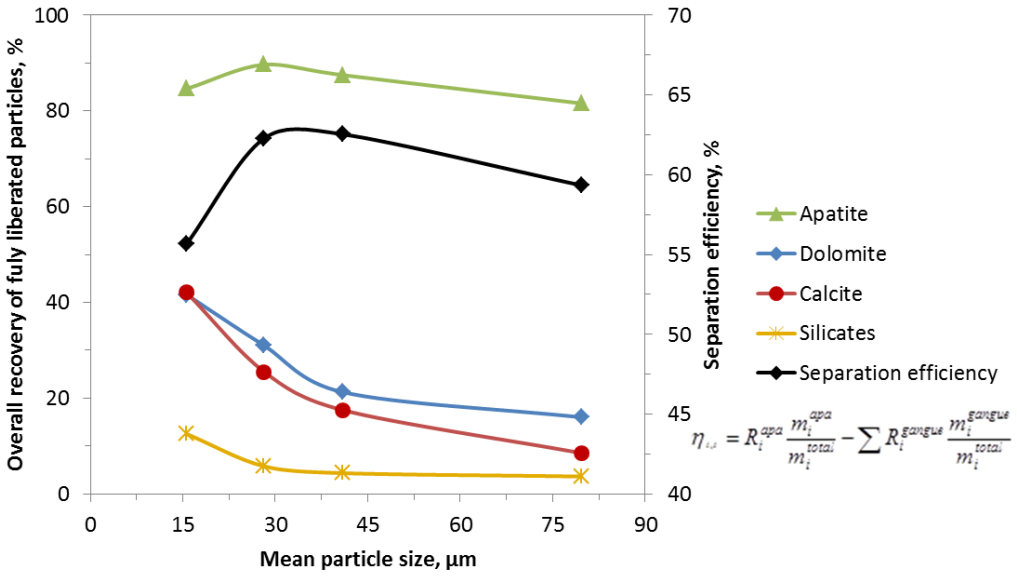

Figure 9. *Recovery as a function of mineral hydrophobicity and size (apatite: strongly floatable, dolomite and calcite: weakly floatable, and silicates mineral recovered by entrainment)*

3.3 Effect of some hydrodynamics variables

3.3.1 Flotation results

The main flotation parameters with a strong influence on the turbulent hydrodynamics were investigated, including different types of impellers, air flow rate, impeller tip velocity and pulp density.

The different impeller-stator systems with the same diameter and impeller speed provide different suspension states and turbulent dispersions related to the mixing of particles in the

pulp. Applying the double finger type impeller (DF) produces a better apatite recovery and also grade compared the Outukumpu type impeller (OK) (cf. **Figure 10a**).

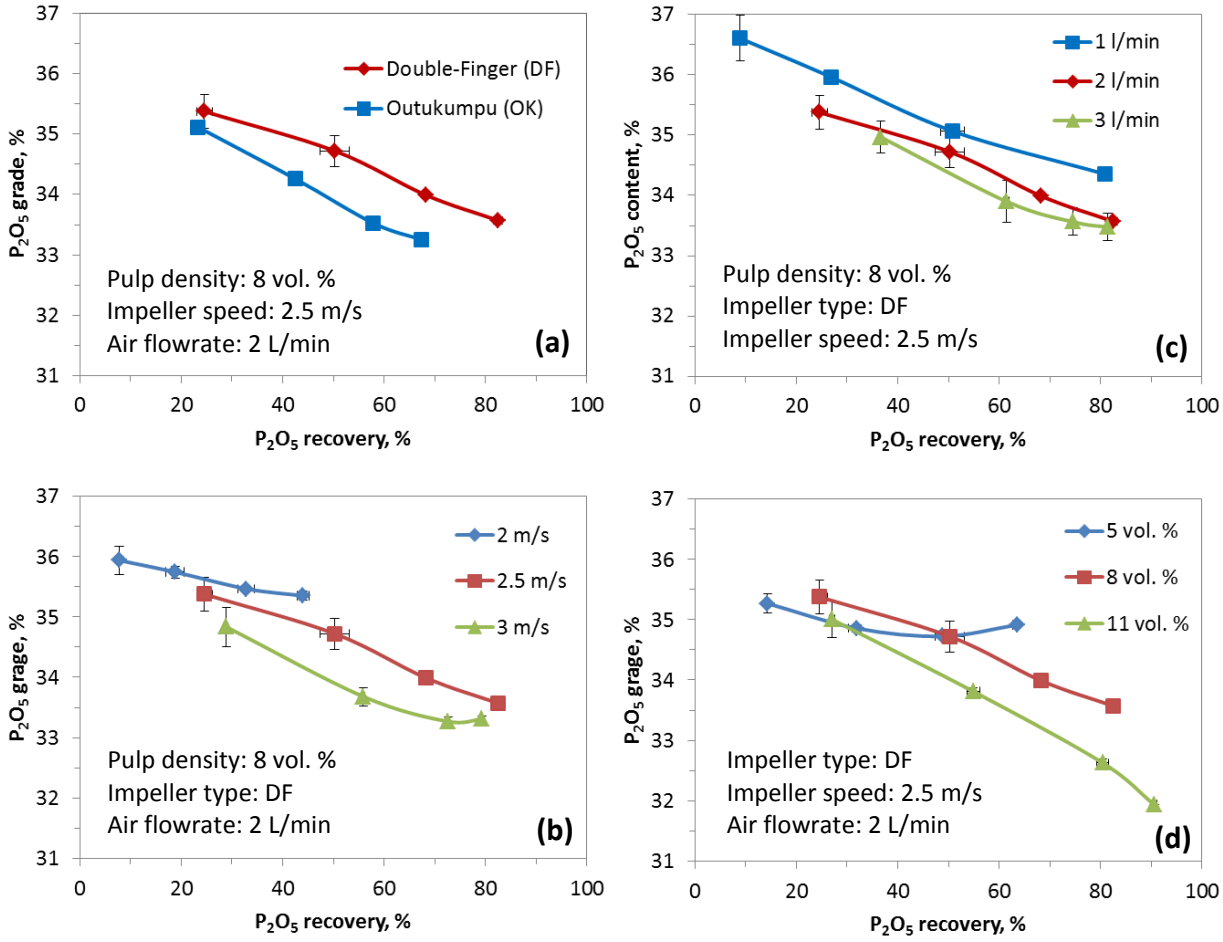

Figure 10. *Effect of some hydrodynamics parameters* ***a)*** *impeller type effect at 8 vol.%, 2.5 m/s impeller speed and 2 L/min of air flowrate,* ***b)*** *impeller speed effect at 8 vol.%, double finger impeller and 2 L/min of air flowrate,* ***c)*** *air flowrate effect at 8 vol.%, double finger impeller and at 2.5 m/s tip speed,* ***d)*** *pulp density effect at 2 L/min of air flowrate, double finger impeller and 2.5 m/s impeller speed*

Figure 10b shows the effects of impeller speed, where a lower speed (low energy dissipation rates) is the reason for the incomplete suspension. The 1s-criterion is used to describe the conditions required to maintain the solids in suspension [33-35], i.e. a situation below the 1s criterion will negatively affect the dispersion of aggregates within the pulp. This leads to a decrease in the collision frequency between bubbles and particles, thus lowering the flotation kinetics. The impeller types/speeds (energy dissipation rate) are important due to the fact that they determine the frequency of collision between particles and bubbles [36-39] and are also the cause of detachment of coarser particles [40, 41].

As the pulp density (solids volume percent) increases (high N_b), so does the energy dissipation, thus a higher recovery and faster flotation kinetics of the valuable minerals can be expected (cf. **Figure 10d**). However, there are also negative rheological effects within the

pulp which result in an increase in entrainment of fine gangue particles, thus negatively influencing the grade.

The influence of the air flow rate on the flotation is shown in **Figure 10c**. With a decrease in the air flowrate, the grade-recovery curve shifts to the upper right corner, however negatively affecting the flotation kinetics. Indeed, the particles float slower, but the grade is highly affected due to less entrainment at the low air flow rate. Furthermore, as the air flow rate increases, so does the kinetics of the particles while still reaching an asymptote. This means that it is useless to keep increasing the airflow rate in the hope of floating faster and better.

For air flow rate, impeller speed and pulp density, the grade generally increases with a decrease in those parameters, which also leads to a decrease in flotation rate constant. In contrast, as these parameters increase, an increase in recovery can be seen as well.

The results were achieved with only one rougher flotation stage, yet these trends would also be useful to improve grade or recovery for each flotation stages (rougher, scavengers and cleaners).

The relationship between turbulent hydrodynamic variables and flotation kinetics depends not only on the pulp phase (suspension state) but also on the froth properties, i.e. froth stability, froth structure and bubble size d_b, which are influenced by the impeller types/speed, the air flowrate and the pulp density.

3.3.2 Experimental and predicted flotation kinetics

Assuming a first-order kinetics model, the recovery was fitted assuming a first-order kinetics applies. Therefore, the following model was used:

$$R_t = R_{\max}(1-e^{-kt}) \qquad \textit{(Eq. 2)}$$

where R_t is cumulative recovery up to time t, $R_{\max}$ is cumulative ultimate recovery (at an infinite time) and k is the flotation rate.

A nonlinear least square regression was applied to calculate experimental flotation rate constants $k_{\exp}$ from the best fit of the curve of experimental recoveries versus flotation time using **Eq. 2**.

The pulp flotation kinetics model (excluding froth recovery) of Pyke et al. [42, 43] is used to calculate (predict) flotation rate constants [20].

$$k_{pulp} = 2.39.\frac{\dot{V}_g}{d_b V_{cell}}\left[0.33\frac{\varepsilon^{4/9} d_b^{7/9}}{\upsilon^{1/3}}\left(\frac{\Delta\rho_i}{\rho_F}\right)^{2/3}\frac{1}{v_b}\right]E_c E_a (1-E_d) \qquad \textit{(Eq. 3)}$$

where $\dot{V}_g$ - volume gas flow rate, V_{cell} - volume of the flotation cell, d_b - bubble Sauter mean diameter, $\Delta\rho_i$ - the difference between the particle and fluid densities, v_b - velocity of bubbles, υ - kinematic viscosity of the fluid, ε - energy dissipation rates, ρ_F - specific gravity of the fluid, E_c, E_a, E_d - collision, attachment and detachment efficiencies.

The net power input P was measured as it can be used to estimate the energy dissipation rate ε and power number (also known as Newton number) c_P in a flotation cell [44]. **Figure 11** shows the linear relationship between the flotation rate constant and mean energy dissipation rate $\bar{\varepsilon}$. The flotation process takes place under turbulent conditions [45], therefore, the energy dissipation strongly affects the flotation kinetics.

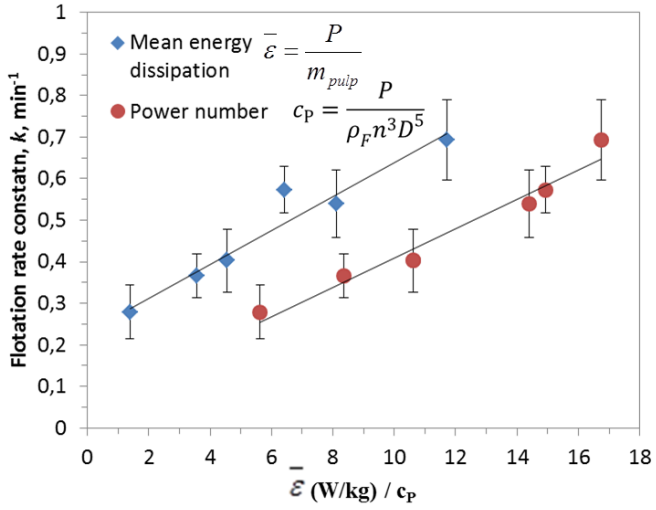

Figure 11. *Flotation rate constant as a function of mean energy dissipation rate and power number (the flotation rate constants were calculated using* ***Eq. 2*** *based on the apatite recoveries from* ***Figure 10****)*

Figure 12 shows the comparison between the experimental and calculated flotation rate constant. The results show a very good correlation, however, the calculated flotation rate constants are larger than the experimental ones. This is because of froth phase effects.

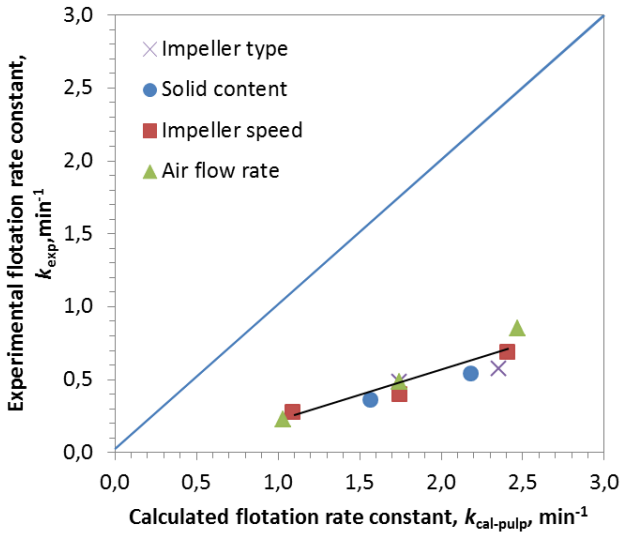

Figure 12. *Predicted flotation rate constant ($k_{cal-pulp}$) vs. Experimental values (d_b =41.2x10^{-3} m; E_a =0.0115; E_d =0; V_{cell} =1.1x10^{-3} m^3; ρ_p =3.10 g/cm^3, E_c calculated using* ***Eq. 1****)*

To date, most of the models were developed based on sulfide ores (low grade), the changing of pulp properties is neglected in this model. In this study, the lab-scale flotations of rich apatite ores with a high mass pull (fast flotation kinetics) lead to severe changes in pulp properties (particular the pulp density) and also froth properties. The effects of the froth layer, especially froth depth is not taken into account in this case. To develop the flotation kinetics model in case of such rich apatite ores containing calcium minerals is thus the aim of the on-going research.

4 Conclusions

An automated mineralogy MLA was applied based on two-dimensional SEM to investigate the characteristics size-by-size of the feed, concentrates and tailings as well. The following conclusions could be made:

- The carbonates minerals constitute the main gangue and are finely intergrown with apatite. Because of similar surface properties for both minerals, reagents can interact with carbonate minerals which have weakly hydrophobic surface properties. Fully liberated carbonate particles can be float but did not float as well as the ones that were associated with apatite.
- The effect of size and liberation for different minerals hydrophobicity shows a strong influence on flotation performance.
- The recovery of the hydrophilic minerals group shows the effect of size on the entrainment.

Furthermore, some hydrodynamics variables were investigated to help understanding the important role of turbulence, especially for fine particle flotation process. This can be useful information to design the hydrodynamics conditions for different flotation stages and particles size as well.

In addition, the comparison between the experimental and predicted flotation rate constants indicated that the froth phase should be taken into account in the model. This is a big challenge, especially in case of flotation of carbonaceous apatite.

Acknowledgements

The authors would like to thank Thomas Heinig and Sabine Haser for their support, discussions and also conducting some of the MLA measurements, Yvonne Volkmar, for conducting ICP-OES measurements. Further thanks go to Dr. Thomas Leissner from the Institute of Mechanical Process Engineering and Mineral Processing, TU Bergakademie Freiberg for his support and discussions. We thank Bruno Michaux for his discussion, which improved the manuscript.

We would like to acknowledge Nguyen Quoc Nghiep from the Vietnam Apatite Limited Company and Le Viet Ha, Pham Thanh Hai and Dr. Nguyen Hoang Son from the Department of Mineral Processing, Hanoi University of Mining and Geology for apatite ore sample provision and preparation to transport to Germany.

Finally, I would like to thank the Vietnam International Education Development (VIED) - Ministry of Education and Training (MOET) for financial support through the 911 scholarship.

References

1. FAO, *World fertilizer trends and outlook to 2020.* Food and agriculture organization of the united nations, 2017.
2. Zapata, F. and R.N. Roy, *Use of phosphate rocks for sustainable agriculture.* Food and Agriculture Organization of the United Nations, 2004.
3. Oelkers, E.H. and E. Valsami-Jones, *Phosphate Mineral Reactivity and Global Sustainability.* Elements, 2008. **4**(2): p. 83-87.
4. Komar Kawatra, S. and J.T. Carlson, *Beneficiation of phosphate ore.* Society for Mining, Metallurgy & Exploration, 2014.
5. Abouzeid, A.-Z.M., *Physical and thermal treatment of phosphate ores — An overview.* International Journal of Mineral Processing, 2008. **85**(4): p. 59-84.
6. Baudet, G. and M. Save, *Phosphoric esters as carbonate collectors in the flotation of sedimentary phosphate ores.* 1999: p. 163-185.
7. McCLELLAN, G.H. and S.J. VAN KAUWENBERGH, *Mineralogical and chemical variation of francolites with geological time.* Journal of the Geological Society, 1991. **148**(5): p. 809-812.
8. Somasundaran, P. and D. Wang, *Chapter 4 Mineral–flotation reagent equilibria*, in *Developments in Mineral Processing*, W. Dianzuo, Editor. 2006, Elsevier. p. 73-141.

9. Fuerstenau, D.W. and D.M. Deason, *Effect of Surface Transformation Processes on the Surface Chemistry and Flotation Behavior of Dolomite and Apatite.* XVII International Mineral Processing Congress, 1991. **IV**: p. 71-91.
10. Wiegel, R.L., *Phosphate rock beneficiation practice.* 1999.
11. Save, G.B.a.M., *Phosphoric esters as carbonate collectors in the flotation of sedimentary phosphate ores.* 1999.
12. G. Baudet and M. Save, *Phosphoric esters as carbonate collectors in the flotation of sedimentary phosphate ores.* 1999.
13. B. M. Moudgil and D. Ince, *Effect of sodium chloride on flotation of dolomite from apatite.* 1991.
14. Leistner, T., et al., *A study of the reprocessing of fine and ultrafine cassiterite from gravity tailing residues by using various flotation techniques.* Minerals Engineering, 2016.
15. Leistner, T., U.A. Peuker, and M. Rudolph, *How gangue particle size can affect the recovery of ultrafine and fine particles during froth flotation.* Minerals Engineering, 2017. **109**: p. 1-9.
16. Trahar, W.J. and L.J. Warren, *The flotability of very fine particles — A review.* International Journal of Mineral Processing, 1976. **3**(2): p. 103-131.
17. Trahar, W.J., *A rational interpretation of the role of particle size in flotation.* International Journal of Mineral Processing, 1981. **8**(4): p. 289-327.
18. Dai, Z. and e. al, *Particle-bubble collision models - a review.* Advances in Colloid and Interface Science, 2000: p. 231-256.
19. Luttrell, G.H. and R.H. Yoon, *A hydrodynamic model for bubble-particle attachment.* Journal of Colloid and Interface Science, 1992. **154**(1): p. 129-137.
20. Yoon, R.-H., et al., *Development of a turbulent flotation model from first principles and its validation.* International Journal of Mineral Processing, 2016.
21. Do, H., *Development of a Turbulent Flotation Model from First Principles.* Dissertation, 2010.
22. Sherrell, I.M., *Development of a Flotation rate equation from First Principles under Turbulent flow conditions*. Dissertation. 2004.
23. Wills, B.A. and J.A. Finch, *Chapter 12 - Froth Flotation*, in *Wills' Mineral Processing Technology (Eighth Edition)*. 2016, Butterworth-Heinemann: Boston. p. 265-380.
24. Leißner, T., H.H. Duong, and e. al., *Investigation of mineral liberation by transgranular and intergranular fracture after milling.* International of Mineral Processing Congress, 2016.
25. Leißner, T., et al., *A mineral liberation study of grain boundary fracture based on measurements of the surface exposure after milling.* International Journal of Mineral Processing, 2016. **156**: p. 3-13.
26. Dobby, G.S. and O.N. Savassi, *An Advanced Modelling technique for scale-up of batch flotation results to plant metallurgical performance.* SGS minerals services, 2005.
27. Fandrich, R., et al., *Modern SEM-based mineral liberation analysis.* International Journal of Mineral Processing, 2007. **84**(1-4): p. 310-320.
28. Gu, Y., *Automated Scanning Electron Microscope Based Mineral Liberation Analysis.* Journal of Minerals & Minerals Characterization & Engineering, 2003. **2**.
29. Sandmann, D. and J. Gutzmer, *Use of Mineral Liberation Analysis (MLA) in the Characterization of Lithium-Bearing Micas.* Journal of Minerals and Materials Characterization and Engineering, 2013. **01**(06): p. 285-292.
30. Vianna, S.M.e.a., *The influence of particle size and collector coverage on the floatability of galena particles in a natural ore.* 2003.
31. Weksby BE, S.D.D., *On the Interpretation of Floatability Using the Bubble Load*. 2009, The University of Queensland.
32. Jameson, G.J., *The effect of surface liberation and particle size on flotation rate constants.* Minerals Engineering, 2012. **36–38**: p. 132-137.
33. Nguyen, A.V., et al., *A review of stochastic description of the turbulence effect on bubble-particle interactions in flotation.* International Journal of Mineral Processing, 2016.

34. Schubert, H. and C. Bischofberger, *On the hydrodynamics of flotation machines.* International Journal of Mineral Processing, 1978. **5**(2): p. 131-142.
35. Zwietering, T.N., *Suspending of solid particles in liquid by agitators.* Chemical Engineering Science, 1958. **8**(3): p. 244-253.
36. Schubert, H., *On the turbulence-controlled microprocesses in flotation machines.* International Journal of Mineral Processing, 1999. **56**(1–4): p. 257-276.
37. Schubert, H., *On the optimization of hydrodynamics in fine particle flotation.* Minerals Engineering, 2008. **21**(12-14): p. 930-936.
38. Jameson, G.J. and T. Payne, *The effect of machine hydrodynamics on the flotation rate constant.* Flotation 13, 2013.
39. Bloom, F. and T.J. Heindel, *Mathematical modelling of the flotation deinking process.* Mathematical and Computer Modelling, 1997. **25**(5): p. 13-58.
40. Schulze, H.J., *New theoretical and experimental investigations on stability of bubble/particle aggregates in flotation: A theory on the upper particle size of floatability.* International Journal of Mineral Processing, 1977. **4**(3): p. 241-259.
41. Schulze, H.J., *Dimensionless number and approximate calculation of the upper particle size of floatability in flotation machines.* International Journal of Mineral Processing, 1982. **9**(4): p. 321-328.
42. Pyke, B., D. Fornasiero, and J. Ralston, *Bubble particle heterocoagulation under turbulent conditions.* Journal of Colloid and Interface Science, 2003. **265**(1): p. 141-151.
43. Pyke, B., *Bubble-particle capture in Turbulent Flotation systems.* 2004.
44. Anh V. Nguyen and H.J. Schulze, *Colloidal Science of Flotation*. 2004, New York: Marcel Dekker.
45. Amini, E., *Influence of Flotation Cell Hydrodynamics on the Flotation Kinetics and Scale up of Flotation Recovery*. 2012, The University of Queensland.